

1 This is the peer reviewed version of the following article: Cornacchia L, Wharton G,  
2 Davies G, Grabowski RC, Temmerman S, van der Wal D, Bouma TJ, van de Koppel J. (2020) Self-  
3 organization of river vegetation leads to emergent buffering of river flows and water levels. Proc. R.  
4 Soc. B 287: 20201147. <http://dx.doi.org/10.1098/rspb.2020.1147>. This article may be used for non-  
5 commercial purposes in accordance with the publisher's Terms and Conditions for Self-Archiving.  
6

## 7 **Self-organization of river vegetation leads to emergent buffering** 8 **of river flows and water levels**

### 9 Authors:

10 Loreta Cornacchia <sup>a, f</sup> [Loreta.Cornacchia@nioz.nl](mailto:Loreta.Cornacchia@nioz.nl)  
11 Geraldene Wharton <sup>b</sup> [G.Wharton@qmul.ac.uk](mailto:G.Wharton@qmul.ac.uk)  
12 Grieg Davies <sup>c</sup> [Grieg.Davies@southernwater.co.uk](mailto:Grieg.Davies@southernwater.co.uk)  
13 Robert C. Grabowski <sup>d</sup> [R.C.Grabowski@cranfield.ac.uk](mailto:R.C.Grabowski@cranfield.ac.uk)  
14 Stijn Temmerman <sup>e</sup> [Stijn.Temmerman@uantwerpen.be](mailto:Stijn.Temmerman@uantwerpen.be)  
15 Daphne van der Wal <sup>a, g</sup> [Daphne.van.der.Wal@nioz.nl](mailto:Daphne.van.der.Wal@nioz.nl)  
16 Tjeerd J. Bouma <sup>a, f, h</sup> [Tjeerd.Bouma@nioz.nl](mailto:Tjeerd.Bouma@nioz.nl)  
17 Johan van de Koppel <sup>a, f</sup> [Johan.van.de.Koppel@nioz.nl](mailto:Johan.van.de.Koppel@nioz.nl)  
18  
19

### 20 Affiliations:

21 a: NIOZ Royal Netherlands Institute for Sea Research, Department of Estuarine and Delta Systems, and  
22 Utrecht University, P.O. Box 140, 4400 AC Yerseke, the Netherlands.  
23 b: School of Geography, Queen Mary University of London, London, UK  
24 c: Southern Water Services, Southern House, Worthing, UK  
25 d: Cranfield Water Science Institute, Cranfield University, Cranfield, UK  
26 e: Ecosystem Management Research Group, University of Antwerp, Universiteitsplein 1, 2610  
27 Wilrijk, Belgium  
28 f: Groningen Institute for Evolutionary Life Sciences, University of Groningen, PO Box 11103, 9700 CC  
29 Groningen, The Netherlands  
30 g: Faculty of Geo-Information Science and Earth Observation (ITC), University of Twente, P.O. Box 217,  
31 7500AE, Enschede, The Netherlands  
32 h: Faculty of Geosciences, Department of Physical Geography, Utrecht University, Utrecht, The  
33 Netherlands  
34

### 35 Corresponding author:

36 Loreta Cornacchia  
37 Royal Netherlands Institute for Sea Research  
38 Korringaweg 7  
39 4401 NT Yerseke  
40 The Netherlands  
41 e.mail: [loreta.cornacchia@nioz.nl](mailto:loreta.cornacchia@nioz.nl)  
42 Tel.: +31 (0)113 577 457  
43 Fax: +31 (0)113 573 616  
44

45 Keywords: bio-physical feedbacks | spatial self-organization | flow regulation | submerged aquatic  
46 macrophytes

47 ***Abstract***

48 Global climate change is expected to impact hydrodynamic conditions in stream ecosystems. There is  
49 limited understanding of how stream ecosystems interact and possibly adapt to novel hydrodynamic  
50 conditions. Combining mathematical modelling with field data, we demonstrate that bio-physical  
51 feedback between plant growth and flow redistribution triggers spatial self-organization of in-channel  
52 vegetation that buffers for changed hydrological conditions. The interplay of vegetation growth and  
53 hydrodynamics results in a spatial separation of the stream into densely vegetated, low-flow zones  
54 divided by unvegetated channels of higher flow velocities. This self-organization process decouples  
55 both local flow velocities and water levels from the forcing effect of changing stream discharge. Field  
56 data from two lowland, baseflow-dominated streams support model predictions and highlight two  
57 important stream-level emergent properties: vegetation controls flow conveyance in fast-flowing  
58 channels throughout the annual growth cycle, and this buffering of discharge variations maintains  
59 water depths and wetted habitat for the stream community. Our results provide important evidence of  
60 how plant-driven self-organization allows stream ecosystems to adapt to changing hydrological  
61 conditions, maintaining suitable hydrodynamic conditions to support high biodiversity.

## 62 **Introduction**

63 The importance of vegetation in affecting water and air flow and shaping physical landscapes has  
64 been widely recognized [1, 2]. Mountain and hillslope vegetation reduces surface runoff, river  
65 discharge and erosion rates, thereby affecting landscape morphology [3, 4]; vegetation steers tidal  
66 landscape development [5-7] and dune formation [8]; and in-stream, riparian, and floodplain plants  
67 affect the processes and forms of alluvial rivers [9-11]. Water flow velocities in rivers are a function  
68 of the balance between energy imposed by slope or discharge and the resistance imposed by the river  
69 bed. Within shallow, low-energy rivers, submerged and marginal aquatic vegetation imparts a  
70 resistance to water flow [12] that affects water velocities in the channel [13-15]. Conventional  
71 models, relating river discharge to flow velocity, assume vegetation to be an independent resistance  
72 factor restricting water flow [16] with vegetation cover regarded as a static entity, presuming a uni-  
73 directional effect of vegetation on water flow. However, aquatic vegetation cover is also controlled by  
74 water flow, among other factors (reviewed in [17]); water velocity influences the presence, density  
75 and species composition of aquatic vegetation communities [17, 18]. Whilst field surveys [14, 15] and  
76 models [19] have highlighted the impact of seasonal variation in vegetation cover in streams on local  
77 water velocities, they often ignore the two-way interaction in the process.

78 Aquatic vegetation typically grows as monospecific patches within streams [17] with a  
79 patterning caused by self-organization processes emerging from the divergence of water around  
80 vegetation patches [20]. This interaction results in spatial patterns of patch alignment [21] that are  
81 important for species facilitation [22]. Although self-organization is recognized as an important  
82 regulating process in several natural systems [23], including the morphological structure of fluvial  
83 systems [24], there is insufficient understanding of the implications of self-organization induced by  
84 the interaction between plant growth and water flow for the functioning of vegetated rivers and  
85 streams. Moreover, we know very little about the ability of stream ecosystems to maintain a healthy,  
86 diverse ecosystem in the face of changing discharge. This is a pressing need, as these high-  
87 biodiversity ecosystems are expected to face more severe hydrological conditions due to global  
88 climate change and human modifications of rivers and their catchments.

89           We present a combined mathematical and empirical investigation that reveals how feedback  
90 mechanisms between in-stream plants and river discharge buffer flow velocities and water levels  
91 against high and low flows. A model is developed that describes the interplay of plant growth and  
92 hydrodynamics within a spatially heterogeneous vegetated stream. With this model, we explore how  
93 self-organization processes that emerge from this interaction create heterogeneity in plant biomass  
94 and water flow, and how this in turn affects stream hydrodynamic conditions. We model an “abstract”  
95 stream where we adopt a simplified setting of a single channelized flow area in between two  
96 vegetated areas, and focus on the lateral adjustment of the effective width of the channel in response  
97 to increasing discharge (**Fig. 1A**). Moreover, we assume that the stream is groundwater fed and  
98 baseflow dominated, and hence discharge is presumed to change gradually. Plant growth is described  
99 in the model using the logistic growth equation, and plant mortality due to hydrodynamic stress is  
100 assumed to increase linearly with net water velocity [5]. We assume that the lateral expansion of  
101 plants through clonal growth can be described by a random walk, and we therefore apply a diffusion  
102 approximation [25]. Water flow is modelled using depth-averaged shallow water equations in non-  
103 conservative form. The effects of friction exerted by the bed and vegetation on flow velocity are  
104 represented by the Chézy coefficient, following the approach of Baptist et al. [26], slightly modified  
105 to account for bending of flexible submerged macrophytes in response to increased water flow [27].  
106 To test the model predictions on flow regulation by in-stream plants, we use field measurements of  
107 seasonal variations in plant cover, discharge, water levels and spatial patterns of flow velocities within  
108 and around vegetation patches in two baseflow-dominated single-thread chalk streams with seasonal  
109 variations in discharge. One stream was dominated by mixed submerged and emergent vegetation,  
110 and the other by submerged vegetation (see Materials and methods).

## 111 **Results**

112 **(a) Water discharge regulates vegetation cover.** Our model analysis reveals that the feedback  
113 between vegetation growth and local flow velocity creates a self-organization process that allows  
114 vegetation cover to readjust in response to increasing discharge (see bifurcation analysis in electronic  
115 supplementary material S1 and Fig. S1; electronic supplementary material S2 and Fig. S2). At low

116 discharge, the entire stream becomes homogeneously vegetated (**Fig. 1A**). When discharge increases,  
117 the equilibrium changes from a homogeneously covered state to a partly covered state where the flow  
118 is separated into two distinct spatial zones. One is characterized by low to zero vegetation biomass  
119 and high flow velocities in the middle of the stream, and the other by high biomass and low flow  
120 velocities at the edges of the stream. This is caused by a scale-dependent effect of vegetation on  
121 hydrodynamics where increased flow resistance locally reduces flow velocities in the vegetated  
122 regions, while water flow is diverted and concentrated outside of the vegetation, thereby inhibiting its  
123 expansion. With steadily increasing discharge, the area of channelled flow progressively increases and  
124 the vegetated portions decrease as plants are uprooted, due to the self-organized adjustment of  
125 vegetation cover to incoming discharge, until the system shifts to an unvegetated equilibrium where  
126 no vegetation can persist (**Fig. 1A**). The resulting inverse relationship between incoming flow  
127 discharge and vegetation cover (**Fig. 1B**) was calibrated to best fit the negative relationship observed  
128 in the field for both study sites, showing that vegetation cover decreases (as plants are uprooted) with  
129 increasing discharge ( $R^2 = 0.77$ ,  $p < 0.0001$ , **Fig. 1C**) in response to the seasonal pattern of changing  
130 hydrology and vegetation growth and die-back. Moreover, our model predictions are supported by  
131 experimental evidence of the flow divergence effect of vegetation patches: thus in the zone adjacent  
132 to the vegetation, our model predicts on average a flow acceleration of 52% compared to the  
133 incoming flow velocity, a value close to the 42% average acceleration reported in [20].

134 **(b) Vegetation regulates flow velocities.** The model predicts that local flow velocities both within  
135 the vegetation and in the unvegetated channelled flow area are relatively unaffected by changing  
136 discharge (**Fig. 2A**). The slopes of the velocity-discharge relationships in Fig. 2A indicate that flow  
137 velocities increase by  $0.03 \text{ m s}^{-1}$  per unit increase in discharge within the vegetation, and by  $0.06 \text{ m s}^{-1}$   
138 between the vegetation. This stability in local flow velocities is the consequence of the adjustment of  
139 vegetation cover to increases in overall water discharge, with vegetation expanding when discharge  
140 and flow velocities in the channelled area decrease, and retreating due to uprooting when discharge  
141 and flow velocities increase. Hence vegetation readjustment buffers for increased discharge, thereby  
142 maintaining relatively constant water flow velocities (**Fig. 2A**). These predictions are supported by

143 field data at the two study sites. Flow velocities within and between vegetation patches are buffered  
144 against changes in discharge. The presence of vegetation alone explains up to five times as much of  
145 the variation in the observed flow velocities compared to discharge (electronic supplementary  
146 material S3). In comparison, when averaged over the cross-section, water velocities show a much  
147 stronger response to discharge variations, as a larger volume of water is passing through the channel.  
148 However, since the area covered by vegetation decreases with increasing discharge, the widened,  
149 high-flow section of the stream accommodates the increased discharge and a four-fold increase in  
150 discharge produces only a slight (although significant) increase in local velocities (**Fig. 2B & 2C**;  
151 further details in electronic supplementary material S4 and Fig. S3).

152 **(c) Vegetation regulates water levels.** A second property emerging from the two-way interaction  
153 between water flow and vegetation growth is that water levels in the channel with self-organized  
154 vegetation are maintained at constant level despite increasing discharge (**Fig. 3A**). By increasing  
155 hydraulic roughness, vegetation raises water levels compared to an unvegetated stream for a given  
156 discharge. This effect is most pronounced at low discharge, where water levels are significantly  
157 higher in vegetated compared to unvegetated streams. As discharge increases, however, vegetation  
158 cover decreases, producing strikingly constant water levels, whereas water levels would steadily  
159 increase in a homogeneously vegetated channel (**Fig. 3A**). These predictions are confirmed by our  
160 field measurements of mean water levels from both study sites (**Fig. 3B**). In the ‘mixed vegetation’  
161 site, water levels were on average  $0.28 \pm 0.04$  m, and only increased by 0.09 m for each unit increase  
162 in discharge ( $r^2 = 0.54$ ,  $p = 0.0003$ ; **Fig. 3B**), less than half of what would be expected for an  
163 unvegetated stream (based on the model simulations in Fig. 3A). In the River Frome, the site with  
164 predominantly submerged plants, water levels were on average  $0.39 \pm 0.07$  m, and did not  
165 significantly increase with discharge ( $r^2 = 0.06$ ,  $p = 0.44$ ; **Fig. 3B**), in agreement with model  
166 predictions. Thus, for both study sites the largest effect of vegetation in raising water levels, relative  
167 to an unvegetated stream, occurs at low discharges.

## 168 **Discussion**

169 Using a combined mathematical modelling and empirical study, we show that aquatic macrophytes  
170 can regulate both flow velocities and water levels in baseflow-dominated streams. Regulation results  
171 from a self-organization process caused by the bio-physical feedback between vegetation growth and  
172 flow redistribution. Here, increases in water discharge cause a decrease in partial cover of aquatic  
173 vegetation relative to the unvegetated channels, creating a larger in-channel area for flow conveyance.  
174 This self-organized adaptation of the cover of submerged vegetation buffers the impact of an increase  
175 in discharge, resulting in relatively constant local flow velocities and water levels independent of  
176 discharge. Our study highlights that flow regulation resulting from biophysical feedback mechanisms  
177 and self-organization of aquatic vegetation enables lowland stream ecosystems to adapt to changing  
178 hydrological regimes, such as those induced by global change.

179         The two-way interaction between water flow and plant growth has important implications for  
180 the functioning of the stream as an ecosystem and the provision of a wide range of ecosystem  
181 services. Specifically, it facilitates the maintenance of biodiversity despite increasing discharge that  
182 might otherwise create conditions adverse to plant growth. By buffering variations in local water flow  
183 velocities, vegetation maintains both low-flow-velocity and high-flow-velocity habitats within  
184 individual reaches. This self-organized heterogeneity facilitates ecosystem resilience to discharge  
185 variations and increases stream biodiversity [15, 28] by structuring communities of various aquatic  
186 organisms. In-stream plants increase habitat complexity and maintain a wide range of mesohabitats  
187 for fish species, by providing high-flow areas for feeding and spawning, adjacent to sheltered low-  
188 flow areas for nursery, resting, and refuge from predation. Moreover, by preserving reach-scale water  
189 depths, water temperatures are lowered and can hold greater dissolved oxygen levels [29], and the  
190 high-flow velocities in the channelled areas between vegetation patches increase the turbulent  
191 diffusion of atmospheric oxygen into the water. Thus, the survival of a wide range of aquatic and  
192 riparian organisms is facilitated. This is crucially important during low summer discharge, where  
193 water levels might otherwise be insufficient to maintain a functioning aquatic community [15, 30].  
194 Finally, the creation of fast flowing areas in between the vegetation ensures flow and sediment  
195 conveyance when in-stream macrophyte growth is abundant, maintains river bed permeability by



196 reducing the ingress of fine sediments into river beds [31], and keeps a clean gravel bed as spawning  
197 ground for fish [32].

198 Our model results further highlight two additional important biological implications of the  
199 flow regulation process resulting from self-organization, in terms of the adaptive capacity of fluvial  
200 ecosystems facing altered discharges due to global climate change or human engineering. *First*, our  
201 model predictions indicate that the self-organized vegetation pattern allows vegetation to persist over  
202 a wider range of discharges than if it were homogeneously distributed throughout the river bed. These  
203 non-linear dynamics lead to a metastable equilibrium between plant resistance and fluvial disturbance  
204 in intermediate energy rivers, where the abiotic-biotic feedbacks and self-adjustment processes are  
205 strongest [33, 34]. Moreover, within a certain range of discharge, the system has two stable states, one  
206 where vegetation is patterned and a bare state where vegetation cannot survive (see electronic  
207 supplementary material S1 and Fig. S1). Hence, removal of vegetation due to human management or  
208 natural disturbances under conditions of high discharge might shift the system towards the alternative  
209 unvegetated state, from which vegetation recovery is slow or severely hindered unless discharge is  
210 significantly reduced. A *second* implication of our results is that self-organized pattern formation  
211 strongly increases macrophyte resilience compared to homogeneously vegetated streams, in terms of a  
212 faster recovery of vegetation biomass following, for instance, a disturbance imposed by strong  
213 discharge variations (see electronic supplementary material S5 and Fig. S4). This enhanced resistance  
214 and resilience of stream ecosystems resulting from self-organization processes is highly important in  
215 the light of global change. Intensification of rainfall [35] in combination with land use change in river  
216 catchments [36, 37] may alter hydrologic partitioning and surface runoff, imposing increasingly  
217 stressful and variable discharge conditions on stream ecosystems.

218 Our results, therefore, lead to important considerations for the management of stream  
219 ecosystems. In current maintenance strategies, abundant vegetation growth is typically regarded as  
220 problematic because it decreases the capacity of these streams for water conveyance in response to  
221 high discharge [17, 38]. However, our study provides evidence for the value of submerged aquatic  
222 vegetation in rivers which, through a process of self-organization over time, ensures flow conveyance

223 and maintains sufficient water levels for the aquatic ecological community at low discharges. Hence,  
224 there might be a need to reconsider vegetation as an important component of the adaptive capacity of  
225 stream ecosystems and their ability to maintain a diverse range of habitats. The empirical results in  
226 this study were collected over a 2-year period in two streams that have baseflow-dominated  
227 hydrographs with relatively subtle changes in water discharge. Further research is now needed on  
228 river systems with flashier hydrological regimes and different aquatic plant species (morphologies,  
229 biomechanical properties, and life-history traits) to test the stability and generality of these bio-  
230 physical feedback dynamics. Future studies also need to examine changes over longer (inter-annual)  
231 and shorter (event-based) timescales and explore how changes in river hydrogeomorphology (channel  
232 dimensions, sediment transport) and biogeochemistry (nutrient levels) might impact on the reciprocal  
233 relationships between vegetation and flow properties.

234         Spatial patterning generates important emergent effects (e.g. increased productivity,  
235 resistance) that go beyond the simple creation of heterogeneity, compared with a non-patterned state  
236 [23]. These emergent effects have been increasingly observed in many self-organized ecosystems,  
237 suggesting their generality. The process of water flow diversion within self-organizing ecosystems is  
238 not unique to streams. Similar vegetation-induced self-organization processes affect hydrodynamics  
239 in salt marsh pioneer vegetation [5, 39], diatom-covered tidal flats [40], and flow-governed peat land  
240 ecosystems [23, 41]. This points at the universal emergent properties that result from the interplay of  
241 vegetation, water flow and drainage, shaping the adaptive capacity of fluvial and intertidal ecosystems  
242 and the services these ecosystems deliver in terms of supporting biodiversity. Another implication of  
243 our study is that flow velocities are ultimately determined by the maximum flow stress that plants can  
244 tolerate before being uprooted. Since plant traits are under evolutionary constraints, this might suggest  
245 that physical processes such as water flow can reflect the control of evolutionary processes in bio-  
246 geomorphic systems. With the current rates of climate change threatening ecosystems worldwide and  
247 potentially increasing the frequency and intensity of rainfall, increased insight into the emergent,  
248 regulating properties of spatial self-organization in ecosystems and an understanding of their role in

249 ecosystem resilience will be essential to help maintain natural ecosystems in a future governed by  
 250 global change.

## 251 **Materials and methods**

252 **(a) Model description.** To study how vegetation affects flow velocity and water levels in streams, we  
 253 constructed a spatially-explicit mathematical model of the interplay of plant growth and water flow  
 254 through a heterogeneously vegetated stream. The model consists of a set of partial differential equations,  
 255 where one equation describes the dynamics in two spatial dimensions of plant density ( $P$ ), and where  
 256 water velocity and water level are described using the shallow water equations. By only including the  
 257 essential aspects of the coupling between hydrodynamics and vegetation, our model allows us to  
 258 investigate the key process of flow velocity and water level regulation by macrophytes.

259 The rate of change of plant biomass  $P$  [g DW m<sup>-2</sup>] in each grid cell is described by:

$$\frac{\partial P}{\partial t} = rP \left(1 - \frac{P}{k}\right) - m_w P |u| + D \left( \frac{\partial^2 P}{\partial x^2} + \frac{\partial^2 P}{\partial y^2} \right) \quad (1)$$

260 Here, plant growth is described using the logistic growth equation, where  $r$  [day<sup>-1</sup>] is the intrinsic growth  
 261 rate of the plants and  $k$  [g DW m<sup>-2</sup>] is the plant carrying capacity, that indirectly reflects the mechanisms  
 262 of nutrient and light competition between the plants (see Franklin *et al.* [17] for a review of the main  
 263 factors controlling macrophyte growth and survival). Plant mortality caused by hydrodynamic stress is  
 264 modelled as the product of the mortality constant  $m_w$  [m<sup>-1</sup>] and net water speed [m s<sup>-1</sup>] due to plant  
 265 breakage or uprooting at higher velocities [5, 17, 42]. As the net water speed is converted in m day<sup>-1</sup>,  
 266 the mortality constant is divided by a conversion factor of 86400 to obtain plant mortality in the units  
 267 of g DW m<sup>-2</sup> day<sup>-1</sup>. We assume that the lateral expansion of plants through clonal growth can be  
 268 described by a random walk, and we therefore apply a diffusion approximation, where  $D$  [m<sup>2</sup> day<sup>-1</sup>] is  
 269 the diffusion constant of the plants [25].

270 Water flow is modeled using depth-averaged shallow water equations in non-conservative form [43].

271 To determine water depth and speed in both  $x$  and  $y$  directions we have:

$$\frac{\partial u}{\partial t} = -g \frac{\partial H}{\partial x} - u \frac{\partial u}{\partial x} - v \frac{\partial u}{\partial y} - \frac{g}{C_d^2} u \frac{|u|}{h} + \nabla(D_U \nabla u) \quad (2)$$

$$\frac{\partial v}{\partial t} = -g \frac{\partial H}{\partial y} - u \frac{\partial v}{\partial x} - v \frac{\partial v}{\partial y} - \frac{g}{C_d^2} v \frac{|u|}{h} + \nabla(D_U \nabla v) \quad (3)$$

$$\frac{\partial h}{\partial t} = -\frac{\partial}{\partial x}(uh) - \frac{\partial}{\partial y}(vh) \quad (4)$$

272 where  $u$  [ $\text{m s}^{-1}$ ] is water velocity in the streamwise (x) direction,  $v$  [ $\text{m s}^{-1}$ ] is the water velocity in the  
 273 spanwise (y) direction,  $H$  [m] is the elevation of the water surface (expressed as the sum of water depth  
 274 and the underlying bottom topography),  $h$  [m] is water depth and  $C_d$  [ $\text{m}^{1/2}/\text{s}$ ] is the Chézy roughness  
 275 coefficient due to bed and vegetation roughness and the terms  $\nabla(D_U \nabla u, \nabla v)$  represent turbulent  
 276 diffusion (with  $\nabla = (\frac{\partial}{\partial x}, \frac{\partial}{\partial y})$ ) and horizontal eddy viscosity  $D_U = 0.02 \text{ m}^2 \text{ s}^{-1}$ ). The effects of bed and  
 277 vegetative roughness on flow velocity are represented by determining hydrodynamic roughness  
 278 characteristics for each cover type separately using the Chézy coefficient, following the approach of  
 279 Straatsma and Baptist [44] and Verschoren *et al.* [27].

280 The Chézy coefficient within the unvegetated cells of the simulated grid, which we will refer to as  $C_b$   
 281 in this paper, is calculated using Manning's roughness coefficient through the following relation:

$$C_b = \frac{1}{n} h^{1/6} \quad (5)$$

282 where  $n$  [ $\text{s}/\text{m}^{1/3}$ ] is Manning's roughness coefficient for an unvegetated gravel bed channel and  $h$  [m] is  
 283 water depth.

284 The Chézy coefficient for each grid cell occupied by submerged vegetation, which we will refer  
 285 to as  $C_d$ , is calculated using the equation of Baptist *et al.* [26] and slightly modified by Verschoren *et*  
 286 *al.* [27] to account for reconfiguration of flexible submerged macrophytes. Due to the important  
 287 feedback effects taking place between macrophyte growth and flow velocity [17], we link the  
 288 hydrodynamic and plant growth model by relating wetted plant surface area to plant biomass, to express  
 289 vegetation resistance as:

$$C_d = \sqrt{\frac{1}{C_b^{-2} + (2g)^{-1} D_c A_w}} + \frac{\sqrt{g}}{k_v} \ln \frac{h}{H_v} \quad (6)$$

290 where  $C_b$  [ $\text{m}^{1/2}/\text{s}$ ] is the Chézy coefficient for non-vegetated surfaces (Eq. 5),  $g$  is acceleration due to  
 291 gravity ( $9.81 \text{ m s}^{-2}$ ),  $D_c$  [-] is a species-specific drag coefficient,  $A_w$  [ $\text{m}^2 \text{ m}^{-2}$ ] is the wetted plant surface

292 area (total wetted surface area of the vegetation per unit horizontal surface area of the river [27, 45]),  
293 directly related to plant biomass through the empirical relationship described for *Ranunculus* in Gregg  
294 and Rose [46],  $k_v$  is the Von Kármán constant (0.41 [-]), and  $H_v$  [m] is the deflected vegetation height  
295 (further defined below). The equation proposed by Baptist *et al.* [26] has been identified as one of the  
296 best fitting model to represent the effects of vegetation on flow resistance, for both artificial and real  
297 (submerged and emergent) vegetation [47]. Deflected vegetation height varies as a function of incoming  
298 flow velocity, due to the high flexibility of submerged aquatic vegetation and reconfiguration at higher  
299 stream velocities [45, 48]. Following the approach of Verschoren *et al.* [27],  $H_v$  is calculated within  
300 each vegetated grid cell as the product of shoot length  $L$  [m] and the sine of the bending angle  $\alpha$   
301 [degrees] (**Table 1**), using an empirical relationship between bending angle and incoming current  
302 velocity based on flume experiments performed on single shoots of *Ranunculus penicillatus* [49]. In  
303 our model, bending angle of a single shoot is used to represent the bending angle of a whole patch, as  
304 plants located at the leading edge tend to push the whole canopy towards the stream bed. However,  
305 bending of the vegetation in a patch with multiple shoots can be expected to decrease with increasing  
306 along-stream distance within the patch, due to flow deceleration effects of the vegetation. **Table 1**  
307 provides an overview of the parameter values used, their interpretations, units and sources. We were  
308 able to obtain parameter values from the literature for all parameters except for  $r$ ,  $m_w$  and  $D$ , which  
309 were fine-tuned to provide the best quantitative fit to the observed vegetation cover across the discharge  
310 gradient. The diffusion rate of plants  $D$ , corresponding to an expansion rate of  $8.5 \text{ cm}^2 \text{ day}^{-1}$ , falls within  
311 the range of values reported in [50] ( $2 - 150 \text{ cm}^2 \text{ day}^{-1}$ ). Although our model is principle-seeking and  
312 does not aim to generate precise predictions, the robustness of the model for changes in these parameter  
313 values is presented in electronic supplementary material S6. Sensitivity analyses revealed that changes  
314 in these parameter values resulted in quantitative but not qualitative changes in model behaviour, i.e.  
315 the absolute values of flow velocity changed (quantitative changes), but their relationship with  
316 discharge (trend of relatively constant velocities) remained unchanged. For parameter values outside of  
317 the range tested here, numerical instabilities would arise and produce curvatures in the unvegetated  
318 middle channel, an aspect that was out of the focus of this work and was not investigated further.

319 **(b) Study sites.** Two lowland, groundwater-fed chalk stream reaches were chosen for a two-year  
320 survey of macrophyte growth and flow velocity patterns (**Table 2** and electronic supplementary  
321 material, Fig S5). The first reach, on the Bere Stream (50° 44' 11.50" N, 2° 12' 21.42" W), was  
322 located within the River Piddle catchment. The second reach, Frome Vauchurch (50° 46' 29.95" N, 2°  
323 34' 18.32" W), was located within the River Frome catchment. Based on the river classification in  
324 Rinaldi *et al.* [51], the study sites are single-thread alluvial channels on intermediate (gravel-sand)  
325 substrates with straight-sinuuous planform, characterized by an unconfined, low energy setting and  
326 groundwater-dominated hydrographs. The two study reaches were selected to provide a comparison in  
327 terms of species richness of aquatic macrophyte cover. The Bere Stream reach was selected for its  
328 richness in macrophyte cover, while the Frome Vauchurch reach was dominated by *Ranunculus*  
329 stands. The study reaches were straight sections of 30 m long by 7-9 m wide. In the Bere Stream  
330 ('mixed vegetation site'), the dominant in-channel aquatic macrophyte was water crowfoot  
331 (*Ranunculus penicillatus* subsp. *pseudofluitans*), represented in both floating-leaved and submergent  
332 forms, whilst the stream margins were mainly colonized by the emergent macrophyte *Nasturtium*  
333 *officinale* (watercress) in similar proportions (bar plot in Fig. 2B). Other macrophyte species, such as  
334 *Apium nodiflorum* and *Callitriche* sp., were also present in the channel in sparser stands. In the Frome  
335 Vauchurch ('dominant submerged site'), *Nasturtium* was not found and *Ranunculus* was the dominant  
336 in-stream macrophyte, representing more than 80% of the total macrophyte cover (bar plot in Fig.  
337 2C).

338 **(c) Field measurements.** The two study reaches were mapped throughout two annual growth cycles  
339 (July 2008 – July 2010). Field surveys were conducted monthly from July 2008 to July 2009, and  
340 bimonthly until July 2010. During each survey, macrophyte distribution and hydrodynamic conditions  
341 were mapped along transects that were located at 1-m distance intervals along the 30-m long study  
342 reaches. Along each transect, measurement points were located at 0.5 m intervals to measure water  
343 depth, macrophyte presence and species, and water flow velocities ( $\text{m s}^{-1}$ ) (see electronic  
344 supplementary material, Fig. S6 for an example of a plotted stream cross-section showing the raw  
345 field measurements). Total water depth was measured as the depth between the water surface and the

346 surface of the gravel bed, using a reinforced meter rule. The velocity in each position was measured  
347 down from the water surface at 60% of the total flow depth with an electromagnetic flow meter  
348 (Valeport Model 801) for 30 seconds, to have an estimate of the depth-averaged flow velocity in the  
349 water column [52]. A single measurement at 60% of the water depth was deemed more suitable for  
350 the survey than multiple measurements (for example at 80% and 20% of the water depth), as the  
351 majority of points measured were generally  $<0.5$  m in total depth [53]. The average flow velocities for  
352 the vegetated and unvegetated sections of the channel were calculated for each survey month, based  
353 on the cover type of each measurement point. The relationship between discharge and cross-sectional  
354 average velocities were calculated for each survey month as the ratio between the measured discharge  
355 ( $\text{m}^3 \text{s}^{-1}$ ) and the cross-sectional area ( $\text{m}^2$ ). For comparison, in the main text we present a subset of the  
356 monthly measurements from the ‘dominant submerged’ site that fall within the same range of  
357 discharge as the ‘mixed vegetation’ site. The full dataset is provided in electronic supplementary  
358 material S4 and Fig. S3.

359 **(d) Statistical analyses.** The mean vegetated and unvegetated flow velocities for each survey month  
360 were compared using Kruskal-Wallis one-way tests. The correlations between channel discharge and  
361 mean total water level, and between discharge and vegetated and unvegetated flow velocities in the  
362 ‘mixed vegetation’ site, were tested with a linear regression model. The correlation between channel  
363 discharge and vegetated and unvegetated flow velocities in the ‘dominant submerged’ site was tested  
364 with piecewise regression.

365 **(e) Numerical implementation.** We investigated vegetation development with two-dimensional  
366 numerical simulations using the central difference scheme on the finite difference equations. The  
367 simulated area consisted of a rectangular grid of  $600 \times 250$  cells, to simulate a straight channel (50 m  
368 long, 15 m wide) with rectangular cross-sectional shape and initial bed slope of  $0.0007 \text{ m m}^{-1}$ . The  
369 grid resolution was higher in the spanwise than in the streamwise direction ( $\Delta x = 0.08 \text{ m}$ ,  $\Delta y = 0.06$   
370 m), as the model predictions revealed only lateral (spanwise) variations in vegetation cover and not in  
371 the streamwise direction. Moreover, the grid resolution and the turbulent eddy viscosity ( $D_U = 0.02 \text{ m}^2$   
372  $\text{s}^{-1}$ ) were chosen to obtain numerically stable solutions according to the mesh Peclet number and the

373 Courant-Friedrichs-Lewy condition [54]. The grid resolution had limited effect on the solution of the  
374 model. Simulations performed with a higher spatial resolution ( $\Delta x = 0.04$  m,  $\Delta y = 0.03$  m, a grid of  
375  $1200 \times 500$  cells) showed less than 1% difference in the predicted vegetation cover, water level and  
376 flow velocity estimation. The boundary condition downstream was a constant discharge. No flow was  
377 assumed through the lateral boundaries and thus the velocity component in the direction normal to the  
378 boundary (i.e. cross-stream ( $y$ ) direction) was set to zero. Although a no-slip boundary condition  
379 would be more appropriate to represent bank roughness at the channel edges, it would have required  
380 to properly resolve the boundary layer profile, which was out of the scope of our simplified flow  
381 model. As flow redistribution processes and the scale-dependent feedback leading to vegetation  
382 adjustments mostly occur in the cross-stream direction, we assumed that lateral expansion of  
383 vegetation would be mainly affected in the cross-channel direction, rather than along, the channel.  
384 Therefore, although the model can simulate vegetation growth in both the streamwise and cross-  
385 stream direction, the starting conditions were homogeneous in the streamwise direction: at the  
386 beginning of each simulation, vegetation was set to occupy a fixed amount of the channel bed, in the  
387 form of two bands located along the channel margins and each occupying  $1/3$  of the cross-section (see  
388 electronic supplementary material Fig. S7 for a visualization of the spatial model output). The final  
389 vegetated state was independent of the initial conditions, as was found in other self-organization  
390 models [40, 55]. Simulations where the initial vegetation cover was increased in 10% increments  
391 resulted in the same final vegetation cover.

392 An iterative procedure was used to solve the two equations for flow velocity and vegetation  
393 biomass. The model simulation started with setting initial conditions for  $u$ ,  $v$ , and  $P$ . The streamwise  
394 velocity  $u$  was set to a uniform velocity of  $0.14$  m s<sup>-1</sup> and the spanwise velocity  $v$  was set equal to  
395 zero. The biomass  $P$  was set to  $200$  g m<sup>-2</sup> in the two bands along the channel margins. First, the net  
396 water speed was calculated based on the initial conditions for  $u$  and  $v$ . The net water speed was then  
397 used to calculate the bending angle of the vegetation and the deflected vegetation height ( $H_v$ ). Based  
398 on the initial values of plant biomass  $P$  at the start of the simulation ( $t_0$ ), the vegetative Chézy  
399 roughness was calculated. The change in the water flow velocity in both  $u$  and  $v$  directions was then  
400 calculated based on the Chézy roughness. Finally, given the flow velocities in  $u$  and  $v$ , the changes in



401 plant biomass  $P$  were calculated. The use of a small time step minimized the effect of computation  
402 order on the results. The time step length was set at  $dt = 0.01$  days and the end time of the simulation  
403 was set at 500 days. All presented simulations generally reached equilibrium at  $t = 100$  days. A  
404 simulation was considered to have reached equilibrium when the rate of change of plant biomass over  
405 time was zero ( $dP/dt = 0$ ).

406 A total of 25 simulations were undertaken starting with a discharge value of  $0.57 \text{ m}^3 \text{ s}^{-1}$ . At  
407 the end of each simulation, discharge was progressively increased by  $0.04 \text{ m}^3 \text{ s}^{-1}$  and the results of the  
408 previous simulation were used as initial condition. For each simulation, we calculated the vegetation  
409 cover (% of vegetated cells over the simulated domain), the mean flow velocity in the vegetated cells,  
410 the mean flow velocity in the unvegetated cells, and the mean water depth over the simulated domain.  
411 These values were related to the discharge value in each simulation to produce the relationships in  
412 Figures 1 – 3.

## 413 **Acknowledgements**

414 This work was supported by the Research Executive Agency, through the 7th Framework Programme  
415 of the European Union, Support for Training and Career Development of Researchers (Marie Curie -  
416 FP7-PEOPLE-2012-ITN), which funded the Initial Training Network (ITN) HYTECH  
417 ‘Hydrodynamic Transport in Ecologically Critical Heterogeneous Interfaces’, N.316546. Data  
418 collection in the Frome-Piddle catchment, Dorset, was supported by the Natural Environment  
419 Research Council (algorithm studentship awarded to Grieg Davies) and Queen Mary University of  
420 London (through a university studentship awarded to Bob Grabowski).

## 421 **References**

- 422 1. Dietrich W.E., Perron J.T. 2006 The search for a topographic signature of life. *Nature*  
423 **439**(7075), 411-418.
- 424 2. Corenblit D., Baas A.C., Bornette G., Darrozes J., Delmotte S., Francis R.A., Gurnell  
425 A.M., Julien F., Naiman R.J., Steiger J. 2011 Feedbacks between geomorphology and biota  
426 controlling Earth surface processes and landforms: a review of foundation concepts and  
427 current understandings. *Earth-Science Reviews* **106**(3), 307-331.
- 428 3. Istanbulluoglu E., Bras R.L. 2005 Vegetation-modulated landscape evolution: Effects  
429 of vegetation on landscape processes, drainage density, and topography. *Journal of*  
430 *Geophysical Research: Earth Surface* **110**(F2).

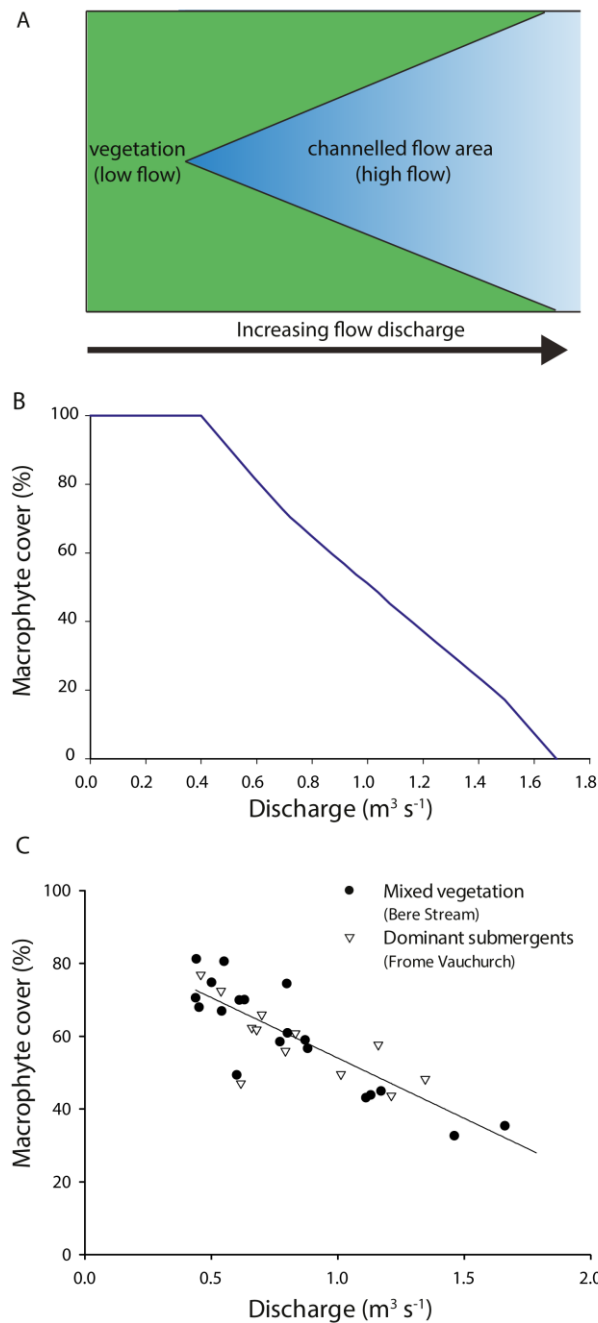
- 431 4. Collins D.B.G., Bras R., Tucker G. 2004 Modeling the effects of vegetation-erosion  
432 coupling on landscape evolution. *Journal of Geophysical Research: Earth Surface* **109**(F3).
- 433 5. Temmerman S., Bouma T., Van de Koppel J., Van der Wal D., De Vries M., Herman  
434 P. 2007 Vegetation causes channel erosion in a tidal landscape. *Geology* **35**(7), 631-634.
- 435 6. Nardin W., Edmonds D.A. 2014 Optimum vegetation height and density for inorganic  
436 sedimentation in deltaic marshes. *Nature Geoscience* **7**(10), 722-726.
- 437 7. Kearney W.S., Fagherazzi S. 2016 Salt marsh vegetation promotes efficient tidal  
438 channel networks. *Nature Communications* **7**.
- 439 8. Baas A., Nield J. 2007 Modelling vegetated dune landscapes. *Geophysical Research*  
440 *Letters* **34**(6).
- 441 9. Tal M., Paola C. 2007 Dynamic single-thread channels maintained by the interaction  
442 of flow and vegetation. *Geology* **35**(4), 347-350. (doi:10.1130/g23260a.1).
- 443 10. Gibling M.R., Davies N.S. 2012 Palaeozoic landscapes shaped by plant evolution.  
444 *Nature Geoscience* **5**(2), 99-105.
- 445 11. Gurnell A. 2014 Plants as river system engineers. *Earth Surface Processes and*  
446 *Landforms* **39**(1), 4-25.
- 447 12. Green J.C. 2005 Modelling flow resistance in vegetated streams: review and  
448 development of new theory. *Hydrological processes* **19**(6), 1245-1259.
- 449 13. Sand-Jensen K. 1998 Influence of submerged macrophytes on sediment composition  
450 and near-bed flow in lowland streams. *Freshwater Biology* **39**(4), 663-679.
- 451 14. Cotton J., Wharton G., Bass J., Heppell C., Wotton R. 2006 The effects of seasonal  
452 changes to in-stream vegetation cover on patterns of flow and accumulation of sediment.  
453 *Geomorphology* **77**(3), 320-334.
- 454 15. Wharton G., Cotton J.A., Wotton R.S., Bass J.A., Heppell C.M., Trimmer M.,  
455 Sanders I.A., Warren L.L. 2006 Macrophytes and suspension-feeding invertebrates modify  
456 flows and fine sediments in the Frome and Piddle catchments, Dorset (UK). *Journal of*  
457 *Hydrology* **330**(1), 171-184.
- 458 16. Chow V.T. 1959 *Open channel hydraulics*. New York, McGraw-Hill Book Co.; 680  
459 p.
- 460 17. Franklin P., Dunbar M., Whitehead P. 2008 Flow controls on lowland river  
461 macrophytes: a review. *Science of the Total Environment* **400**(1), 369-378.
- 462 18. Puijalon S., Bouma T.J., Douady C.J., van Groenendael J., Anten N.P., Martel E.,  
463 Bornette G. 2011 Plant resistance to mechanical stress: evidence of an avoidance-tolerance  
464 trade-off. *New Phytologist* **191**(4), 1141-1149.
- 465 19. Naden P., Rameshwaran P., Mountford O., Robertson C. 2006 The influence of  
466 macrophyte growth, typical of eutrophic conditions, on river flow velocities and turbulence  
467 production. *Hydrological Processes* **20**(18), 3915-3938.
- 468 20. Schoelynck J., De Groote T., Bal K., Vandenbruwaene W., Meire P., Temmerman S.  
469 2012 Self-organised patchiness and scale-dependent bio-geomorphic feedbacks in aquatic  
470 river vegetation. *Ecography* **35**(8), 760-768.
- 471 21. Cornacchia L., Folkard A., Davies G., Grabowski R.C., van de Koppel J., van der Wal  
472 D., Wharton G., Puijalon S., Bouma T.J. 2018 Plants face the flow in V formation: A study of  
473 plant patch alignment in streams. *Limnology and oceanography*.
- 474 22. Cornacchia L., Van Der Wal D., Van de Koppel J., Puijalon S., Wharton G., Bouma  
475 T.J. 2019 Flow-divergence feedbacks control propagule retention by in-stream vegetation:  
476 the importance of spatial patterns for facilitation. *Aquatic Sciences* **81**(1), 17.
- 477 23. Rietkerk M., Van de Koppel J. 2008 Regular pattern formation in real ecosystems.  
478 *Trends in Ecology & Evolution* **23**(3), 169-175.
- 479 24. Phillips C.B., Jerolmack D.J. 2016 Self-organization of river channels as a critical  
480 filter on climate signals. *Science* **352**(6286), 694-697.

- 481 25. Holmes E.E., Lewis M.A., Banks J., Veit R. 1994 Partial differential equations in  
482 ecology: spatial interactions and population dynamics. *Ecology* **75**(1), 17-29.
- 483 26. Baptist M., Babovic V., Rodríguez Uthurburu J., Keijzer M., Uittenbogaard R.,  
484 Mynett A., Verwey A. 2007 On inducing equations for vegetation resistance. *Journal of*  
485 *Hydraulic Research* **45**(4), 435-450.
- 486 27. Verschoren V., Meire D., Schoelynck J., Buis K., Bal K.D., Troch P., Meire P.,  
487 Temmerman S. 2016 Resistance and reconfiguration of natural flexible submerged vegetation  
488 in hydrodynamic river modelling. *Environmental Fluid Mechanics* **16**(1), 245-265.
- 489 28. Stein A., Gerstner K., Kreft H. 2014 Environmental heterogeneity as a universal  
490 driver of species richness across taxa, biomes and spatial scales. *Ecology letters* **17**(7), 866-  
491 880.
- 492 29. Carpenter S.R., Lodge D.M. 1986 Effects of submersed macrophytes on ecosystem  
493 processes. *Aquatic botany* **26**, 341-370.
- 494 30. Hearne J.W., Armitage P.D. 1993 Implications of the annual macrophyte growth  
495 cycle on habitat in rivers. *Regulated Rivers: Research & Management* **8**(4), 313-322.  
496 (doi:10.1002/rrr.3450080402).
- 497 31. Wharton G., Mohajeri S.H., Righetti M. 2017 The pernicious problem of streambed  
498 colmation: a multi-disciplinary reflection on the mechanisms, causes, impacts, and  
499 management challenges. *Wiley Interdisciplinary Reviews: Water*.
- 500 32. Kemp P., Sear D., Collins A., Naden P., Jones I. 2011 The impacts of fine sediment  
501 on riverine fish. *Hydrological Processes* **25**(11), 1800-1821.
- 502 33. Corenblit D., Davies N.S., Steiger J., Gibling M.R., Bornette G. 2014 Considering  
503 river structure and stability in the light of evolution: feedbacks between riparian vegetation  
504 and hydrogeomorphology. *Earth Surface Processes and Landforms* **40**(2), 189-207.
- 505 34. Gurnell A.M., Bertoldi W., Corenblit D. 2012 Changing river channels: The roles of  
506 hydrological processes, plants and pioneer fluvial landforms in humid temperate, mixed load,  
507 gravel bed rivers. *Earth-Science Reviews* **111**(1-2), 129-141.
- 508 35. Houghton J.T., Ding Y., Griggs D.J., Noguera M., van der Linden P.J., Dai X., Maskell  
509 K., Johnson C.A. 2001 *Climate change 2001: the scientific basis*, The Press Syndicate of the  
510 University of Cambridge.
- 511 36. Foley J.A., DeFries R., Asner G.P., Barford C., Bonan G., Carpenter S.R., Chapin  
512 F.S., Coe M.T., Daily G.C., Gibbs H.K. 2005 Global consequences of land use. *Science*  
513 **309**(5734), 570-574.
- 514 37. Palmer M.A., Reidy Liermann C.A., Nilsson C., Flörke M., Alcamo J., Lake P.S.,  
515 Bond N. 2008 Climate change and the world's river basins: anticipating management options.  
516 *Frontiers in Ecology and the Environment* **6**(2), 81-89.
- 517 38. Sukhodolov A.N., Sukhodolova T.A. 2009 Case study: Effect of submerged aquatic  
518 plants on turbulence structure in a lowland river. *Journal of Hydraulic Engineering* **136**(7),  
519 434-446.
- 520 39. Vandenbruwaene W., Temmerman S., Bouma T., Klaassen P., De Vries M.,  
521 Callaghan D., Van Steeg P., Dekker F., Van Duren L., Martini E. 2011 Flow interaction with  
522 dynamic vegetation patches: Implications for biogeomorphic evolution of a tidal landscape.  
523 *Journal of Geophysical Research: Earth Surface* **116**(F1).
- 524 40. Weerman E.J., Van de Koppel J., Eppinga M.B., Montserrat F., Liu Q.X., Herman  
525 P.M. 2010 Spatial Self-Organization on Intertidal Mudflats through Biophysical Stress  
526 Divergence. *The American Naturalist* **176**(1), E15-E32.
- 527 41. Larsen L.G., Harvey J.W., Crimaldi J.P. 2007 A delicate balance: ecohydrological  
528 feedbacks governing landscape morphology in a lotic peatland. *Ecological monographs*  
529 **77**(4), 591-614.

- 530 42. Riis T., Biggs B.J.F. 2003 Hydrologic and hydraulic control of macrophyte  
531 establishment and performance in streams. *Limnology and Oceanography* **48**(4), 1488-1497.
- 532 43. Vreugdenhil C.B. 1989 *Computational hydraulics: an introduction*, Springer Science  
533 & Business Media.
- 534 44. Straatsma M.W., Baptist M. 2008 Floodplain roughness parameterization using  
535 airborne laser scanning and spectral remote sensing. *Remote Sensing of Environment* **112**(3),  
536 1062-1080.
- 537 45. Sand-Jensen K. 2003 Drag and reconfiguration of freshwater macrophytes.  
538 *Freshwater Biology* **48**(2), 271-283.
- 539 46. Gregg W.W., Rose F.L. 1982 The effects of aquatic macrophytes on the stream  
540 microenvironment. *Aquatic botany* **14**, 309-324.
- 541 47. Vargas-Luna A., Crosato A., Uijtewaal W.S. 2015 Effects of vegetation on flow and  
542 sediment transport: comparative analyses and validation of predicting models. *Earth Surface*  
543 *Processes and Landforms* **40**(2), 157-176.
- 544 48. Schoelynck J., Meire D., Bal K., Buis K., Troch P., Bouma T., Meire P., Temmerman  
545 S. 2013 Submerged macrophytes avoiding a negative feedback in reaction to hydrodynamic  
546 stress. *Limnologica-Ecology and Management of Inland Waters* **43**(5), 371-380.
- 547 49. Bal K.D., Bouma T.J., Buis K., Struyf E., Jonas S., Backx H., Meire P. 2011 Trade-  
548 off between drag reduction and light interception of macrophytes: comparing five aquatic  
549 plants with contrasting morphology. *Functional Ecology* **25**(6), 1197-1205.
- 550 50. Sand-Jensen K., Madsen T.V. 1992 Patch dynamics of the stream macrophyte,  
551 *Callitriche cophocarpa*. *Freshwater Biology* **27**(2), 277-282.
- 552 51. Rinaldi M., Gurnell A., Del Tánago M.G., Bussetini M., Hendriks D. 2016  
553 Classification of river morphology and hydrology to support management and restoration.  
554 *Aquatic sciences* **78**(1), 17-33.
- 555 52. Dingman S.L. 1984 *Fluvial hydrology*. New York, 383 pp. WH Freeman, New York;  
556 383 pp. p.
- 557 53. Gordon N.D., McMahon T.A., Finlayson B.L., Gippel C.J., Nathan R.J. 2004 *Stream*  
558 *hydrology: an introduction for ecologists*, John Wiley and Sons.
- 559 54. Vreugdenhil C.B. 2013 *Numerical methods for shallow-water flow*, Springer Science  
560 & Business Media.
- 561 55. Koppel J.v.d., Rietkerk M., Dankers N., Herman P.M. 2005 Scale-dependent  
562 feedback and regular spatial patterns in young mussel beds. *The American Naturalist* **165**(3),  
563 E66-E77.

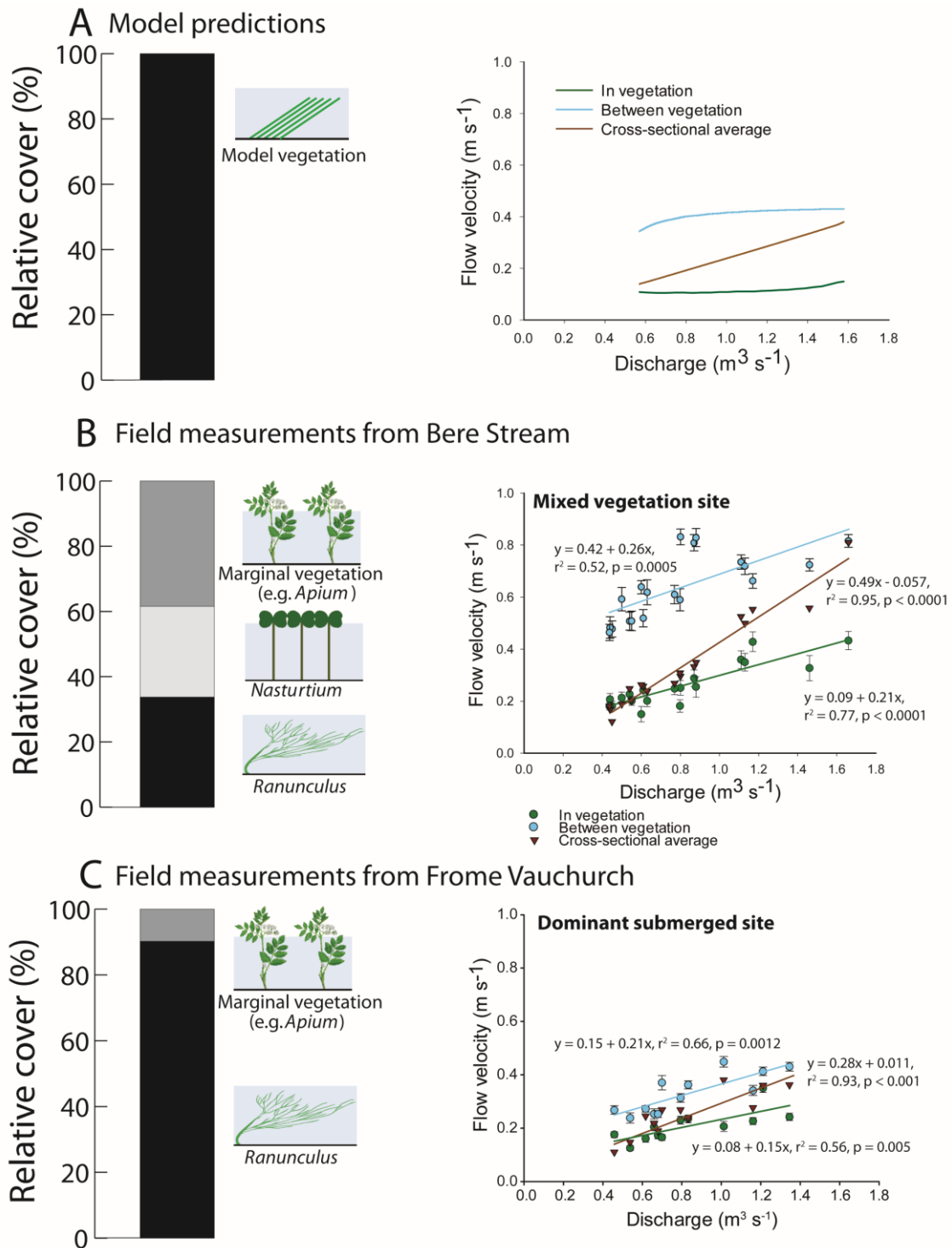
564

565



566  
567  
568  
569  
570  
571  
572  
573  
574  
575

**Fig. 1: Relationship between discharge and macrophyte cover in the model and in two chalk streams. (A)** Schematic diagram of the “abstract” stream simulated in the model: the proportion of the stream cross-section that is vegetated adjusts in response to changes in water discharge. In the model, at very low discharge, the entire stream cross-section is homogeneously vegetated. As discharge increases, the stream becomes spatially separated into densely vegetated, low-flow zones, and low-density, high-flow zones; vegetation cover decreases until the stream becomes entirely unvegetated. **(B)** Relationship between modelled percentage macrophyte cover (fraction of vegetated cells over the whole simulated domain) and discharge. **(C)** Relationship between macrophyte cover and river discharge as found in the field for both study sites ( $N = 31$ ) ( $R^2 = 0.77$ ,  $p < 0.0001$ ).

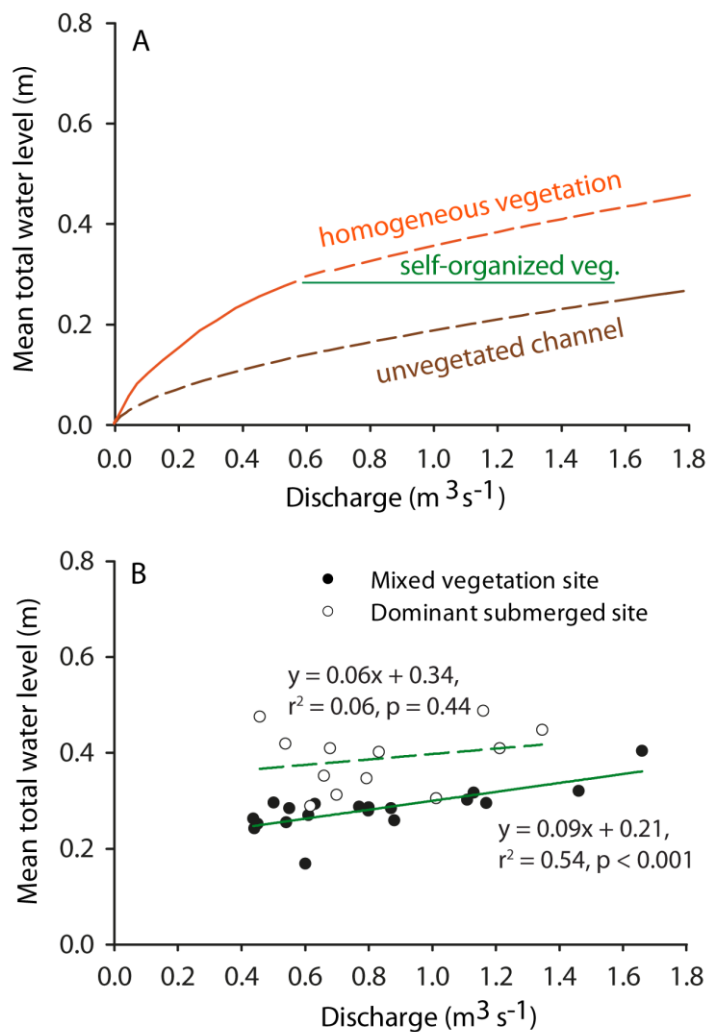


576

577 **Fig. 2: Relationship between discharge and flow velocity in the model and in two chalk streams. (A)**  
 578 *Left:* Schematic representation of the flexible submerged aquatic vegetation considered in the model.  
 579 *Right:* Model predictions of average flow velocities ( $\text{m s}^{-1}$ ) for increasing values of discharge, calculated  
 580 within vegetated and unvegetated sections of the channel, and compared with cross-sectional average flow  
 581 velocities. **(B)** *Left:* Species composition, expressed as relative macrophyte cover (%) per vegetation type,  
 582 at the peak of the growing season (July 2008): marginal vegetation (e.g. *Apium*, emergent along the  
 583 margins), *Nasturtium* (emergent along the margins) and *Ranunculus* (submerged, growing in mid-  
 584 channel). *Right:* relationship between flow discharge ( $\text{m}^3 \text{s}^{-1}$ ) and flow velocity ( $\text{m s}^{-1}$ ) in both vegetated  
 585 and unvegetated river portions in the mixed vegetation site, compared with the cross-sectional average  
 586 flow velocity in the stream. **(C)** *Left:* Species composition, expressed as relative macrophyte cover (%)

587 per vegetation type, at the peak of the growing season (July 2008): marginal vegetation (e.g. *Apium*,  
588 emergent along the margins) and *Ranunculus* (submerged, growing in mid-channel). *Right*: relationship  
589 between flow discharge ( $\text{m}^3 \text{s}^{-1}$ ) and flow velocity ( $\text{m s}^{-1}$ ) in both vegetated and unvegetated river portions  
590 in the dominant submerged site, compared with the cross-sectional average flow velocity in the stream.

591



593

594 **Fig. 3: Relationship between discharge and mean total water level in the model and in two chalk**  
 595 **streams.** (A) Model predictions on the relationship between flow discharge ( $\text{m}^3 \text{s}^{-1}$ ) and water level (m)  
 596 in the simulated channel with vegetation homogeneously distributed over the channel bed (*orange line*),  
 597 with self-organized vegetation (*green line*) and without vegetation (*brown line*). Solid lines indicate the  
 598 dominant state over the range of discharge, and dashed lines indicate the relationship outside that range.  
 599 (B) Field measurements on the relationship between flow discharge ( $\text{m}^3 \text{s}^{-1}$ ) and mean total water level  
 600 (m) in the ‘mixed vegetation’ (*solid green line*) and ‘dominant submerged’ (*dashed green line*) study sites.



601 **Table 1.** Symbols, interpretations, values, units and sources used in the model simulation.

| Symbol   | Interpretation   | Value                             | Unit                             | Source    |
|----------|--|-----------------------------------|----------------------------------|-----------|
| $r$      | Intrinsic growth rate of plants                            | 1                                 | day <sup>-1</sup>                | Estimated |
| $k$      | Carrying capacity of plants                                | 200                               | g DW m <sup>-2</sup>             | [56]      |
| $m_w$    | Plant mortality coefficient due to water shear stress      | 3.8                               | m <sup>-1</sup>                  | Estimated |
| $D$      | Diffusion rate of plants                                   | 0.00085                           | m <sup>2</sup> day <sup>-1</sup> | Estimated |
| $n$      | Manning's roughness coefficient for unvegetated gravel bed | 0.025                             | s/[m <sup>1/3</sup> ]            | [57]      |
| $D_c$    | Drag coefficient   | 0.04                              | Dimensionless                    | [45]      |
| $A_w$    | Wetted plant surface area                                  | $((814.8 * P) - 25.05) * 0.0001$  | m <sup>2</sup> m <sup>-2</sup>   | [46]      |
| $\alpha$ | Bending angle of plants                                    | $15.5 * \sqrt{u^2 + v^2}^{-0.38}$ | degrees                          | [49]      |
| $L$      | Shoot length   | 0.5                               | m                                | [49]      |

602 Note:  $P$  is plant biomass [g DW m<sup>-2</sup>];  $u$  is water velocity in the streamwise (x) direction [m s<sup>-1</sup>];  $v$  is water  
603 velocity in the spanwise (y) direction [m s<sup>-1</sup>].  
604

605 **Table 2.** Location, channel dimensions and flow characteristics of the two study sites.

|   | Bere Stream                       | Frome Vauchurch                   |
|---|-----------------------------------|-----------------------------------|
| Site location                                       | 50° 44' 11.50" N, 2° 12' 21.42" W | 50° 46' 29.95" N, 2° 34' 18.32" W |
| Average discharge (m <sup>3</sup> s <sup>-1</sup> ) | 0.93                              | 1.07                              |
| Peak discharge (m <sup>3</sup> s <sup>-1</sup> )    | 2.5                               | 2.95                              |
| Average width (m)                                   | 7.0                               | 8.9                               |
| Average depth (m)                                   | 0.30                              | 0.42                              |
| Width: depth ratio                                  | 23                                | 21                                |

606

607